Effect of a random noise on scaling laws of finite Prandtl number rotating convection near threshold

D. Laveder,[1] T. Passot,[1] Y. Ponty,[2] and P. L. Sulem[1]

[1]*CNRS, UMR 6529, Observatoire de la Côte d'Azur, Boite Postale 4229, 06304, Nice Cedex 4, France*

[2]*Department of Mathematics, University of Exeter, Exeter EX4 4QE, United Kingdom*

(Received 26 June 1998; revised manuscript received 22 January 1999)

A generalized Swift-Hohenberg model including a weak random forcing, viewed as mimicking the intrinsic source of noise due to boundary defects, is used to reproduce the experimentally observed power-law variation of the correlation length of rotating convection patterns as a function of the stress parameter near threshold, and to demonstrate the sensitivity of the exponent to the amplitude of the superimposed random noise. The scaling properties of rotating convection near threshold are thus conjectured to be nonuniversal.
[S1063-651X(99)51705-4]

PACS number(s): 47.27.Te, 47.20.Lz, 47.52.+j, 47.54.+r

Rotating convection is often viewed as a paradigm for the transition to spatiotemporal chaos because of the destabilization near threshold of straight parallel rolls when the rotation rate τ (defined as the square root of the Taylor number, or twice the Rossby number) exceeds a critical value τ_{KL}. This instability, named after Küppers and Lortz (KL) [1], leads in the weakly nonlinear regime to a time-dependent dynamics with the formation of interpenetrating patches of straight parallel rolls whose directions randomly tilt by an angle close to 60°. Recent laboratory experiments performed at Prandtl number $P=0.93$ and $P=0.83$ in a cylindrical container [2,3] reveal the existence of power laws for the variation of the time average Ξ of the correlation length $\xi=(\langle k^2\rangle-\langle k\rangle^2)^{-1/2}$ with the normalized distance from threshold $\epsilon=(R-R_c)/R_c$. Here $\langle u\rangle=\int u|\hat{W}(\mathbf{k})|^2 d^2\mathbf{k}/\int|\hat{W}(\mathbf{k})|^2 d^2\mathbf{k}$, $\hat{W}(\mathbf{k})$ is the horizontal Fourier transform of the convective mode and $k=|\mathbf{k}|$. Two different power laws are obtained, depending on the magnitude of ϵ: for small ϵ, the measured exponent is close to -0.2, while it approaches -0.75 at larger values of the stress parameter (Fig. 29 in [2], Fig. 18 in [3]), for which the formation of targets whose diameter barely exceeds a wavelength is observed. The first exponent was unexpected since a value -0.5 is predicted by Ginzburg-Landau-type models, at least in the absence of rotation. Numerical simulations of a Swift-Hohenberg (SH) model including rotation in a periodic geometry [4], showed two power laws for Ξ versus ϵ, but with exponents of -0.5 and -1. This model, however, does not include a mean flow and is restricted to large Prandtl numbers.

In this Rapid Communication we address the problem in the framework of a generalized SH model for finite Prandtl number fluids, derived in [5]. Although lateral boundary conditions play an important role in defects generation, we kept periodic boundary conditions in the horizontal directions. Furthermore, very long simulations being required, only moderate resolutions (128×128 or 256×256 collocation points) were used, thus retaining a number of rolls smaller than in the laboratory experiments reported in [2] and [3]. The amplitude W of the temperature or of the vertical velocity mode and the stream function Ψ associated with the horizontal mean flow obey

$$\tau_0\partial_t W=[\epsilon-(\Delta+1)^2]W-\mathcal{N}(W,\Psi) \tag{1}$$

$$[\partial_t-P(\nu+\Delta)]\Delta\Psi=(\boldsymbol{\nabla}\Delta W\times\boldsymbol{\nabla}W)\cdot\hat{\mathbf{z}}+\alpha_6[(\Delta W)^2+\boldsymbol{\nabla}W\cdot\boldsymbol{\nabla}\Delta W]+\alpha_7\Delta(W^2), \tag{2}$$

where $\mathcal{M}=W^2+|\nabla W|^2$ and

$$\mathcal{N}(W,\Psi)=\mathcal{M}W+\alpha_1\boldsymbol{\nabla}W\cdot\boldsymbol{\nabla}\mathcal{M}+\alpha_2(\boldsymbol{\nabla}W\times\boldsymbol{\nabla}\mathcal{M})\cdot\hat{\mathbf{z}}+\alpha_3(\boldsymbol{\nabla}W\times\boldsymbol{\nabla}\Psi)\cdot\hat{\mathbf{z}}.$$

The coefficients τ_0, $\alpha_1,\ldots,\alpha_7$ depend on P and τ. Rigid top and bottom boundary conditions are modeled by the friction coefficient $\nu=\pi^2/q_c^2$ (where q_c denotes the critical wave number) and by the coefficient α_7 which originates from the vertical Reynolds stress. In the absence of rotation, α_2, α_4, α_5, and α_6 vanish, leading to a generalization of Manneville's model [6].

The above system was integrated for $P=1.2$. When sampling the values of the parameters ϵ and τ, a qualitative agreement is obtained with the experimental phase diagram displayed in Fig. 7 of [2], although the curves bounding the various regions are slightly shifted in the model. At small rotation, a direct transition is obtained when increasing ϵ, from straight parallel rolls to spiral-defect chaos [7,8] (the intermediate region corresponding to S-shaped structures requires lateral walls and was obtained in the simulations of the present model in cylindrical geometry [9]). Above the critical rotation τ_{KL}, KL fronts are observed for small values of ϵ, separating domains of straight rolls whose size decreases gradually as ϵ is increased. For larger values of ϵ, the rolls develop a significant curvature and small targets form, like in the experiment [Fig. 1(d)]. A quantitative difference between these two regimes is seen in the time variation of the correlation length displayed in Fig. 2 for $\tau=48$, with $\epsilon=0.1$ and $\epsilon=0.44$. For $\epsilon=0.1$, we observe a few large excursions corresponding to an almost complete ''relaminarization'' of the pattern, where all front defects are eliminated and quasi-straight rolls covering the entire box are formed. These rare events disappear for larger ϵ.

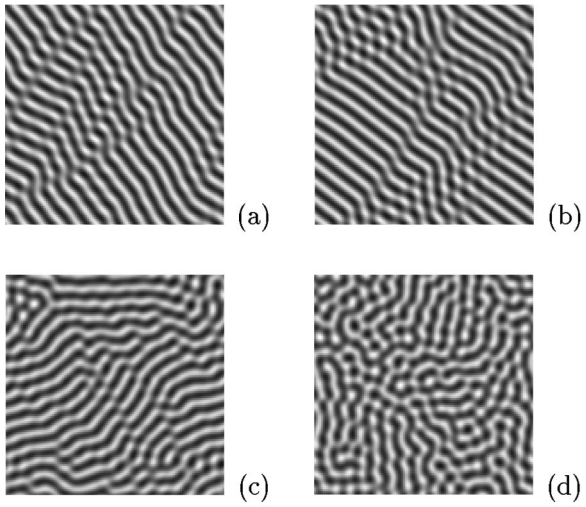

FIG. 1. Convective patterns in the case $\tau=48$ for $\epsilon=0.1$ (a), $\epsilon=0.14$ (b), $\epsilon=0.3$ (c), and $\epsilon=0.44$ (d).

The large excursions seen near threshold can be understood in the context of a three-mode dynamical system of Volterra type [10], where heteroclinic orbits connect three unstable fixed points associated with states of perfectly straight parallel rolls, making an angle of 60° between them. Generic solutions approach these heteroclinic orbits and spend more and more time near the fixed points. This behavior is not observed in the experiments because of the strong sensitivity of such a system to perturbations which, by a small deviation of the trajectory, lead to significant changes in the subsequent evolution. In order to reproduce the continuous destabilization process leading to the successive changes in the orientation of the rolls, a random noise was introduced to prevent trapping [11]. As an alternative, spatial coupling was suggested to be the main source of internal noise in extended systems [12].

Our results are consistent with this picture. The simulations involving only 16 rolls are extremely sensitive to the numerical noise, which at small ϵ affects the time-averaged correlation length Ξ itself. A strong sensitivity to the aspect ratio of the convection cell is also observed: when increasing the resolution of our simulations to 256^2 with $N=32$ rolls,

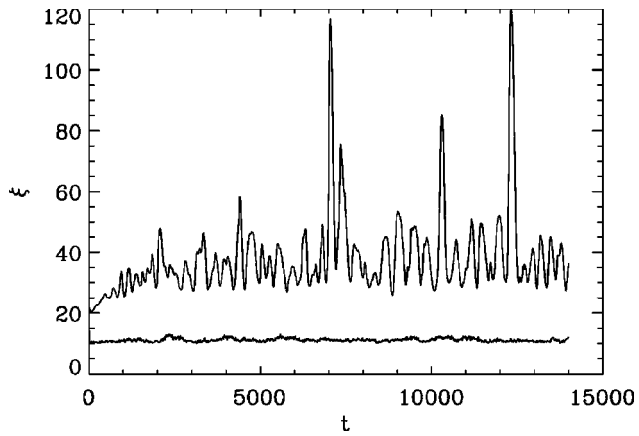

FIG. 2. Time variation of the correlation length ξ for $P=1.2$, $\tau=48$ at $\epsilon=0.1$ (upper curve) and $\epsilon=0.44$ (lower curve) for a number of rolls $N=16$.

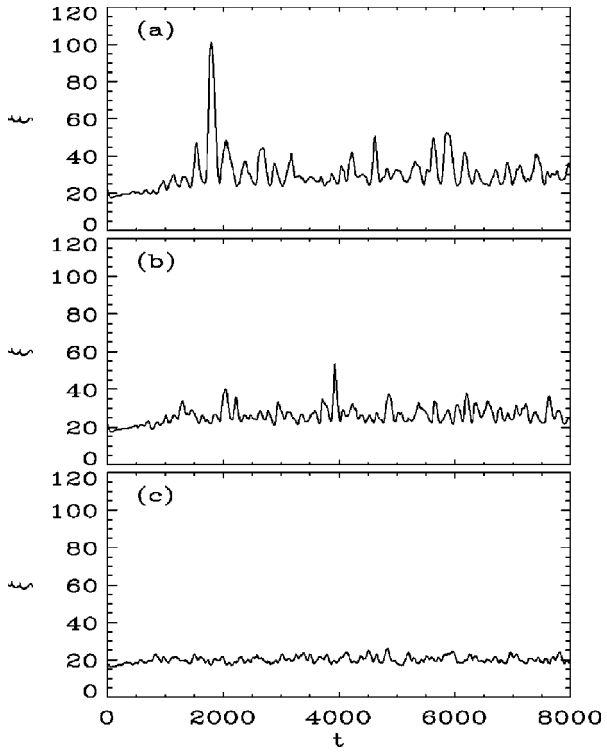

FIG. 3. Time variation of the correlation length ξ for $P=1.2$, $\tau=48$, $\epsilon=0.14$, and $N=16$ rolls for the unperturbed system (a) and in the presence of noise of amplitude 1.25×10^{-4} (b) and 5×10^{-4} (c).

the relaminarization events are almost suppressed [Figs. 3(a) and 4(a)]. Indeed, since the typical distance between front defects depends on ϵ but not on the aspect ratio, increasing the size of the box increases the number of fronts and thus the spatial coupling, which inhibits the relaminarization.

In the simulations with $N=32$, we clearly distinguish an early-time regime characterized by patches of quasi-straight rolls of different orientations interspersed with isolated defects, cellular regions and some small targets [Fig. 5(a)], and a long-time regime during which rolls have a dominant ori-

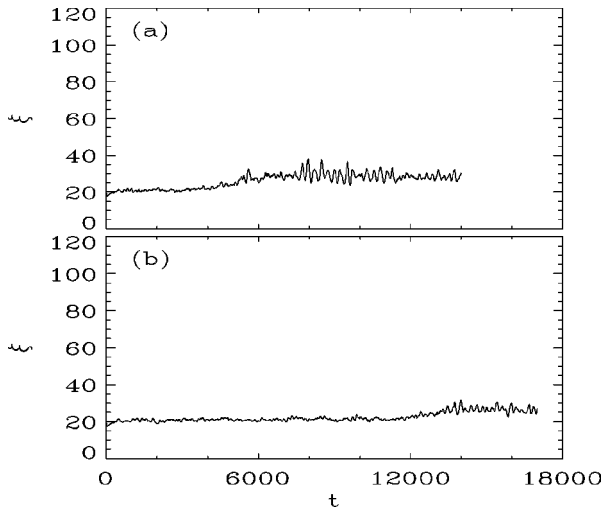

FIG. 4. Time variation of the correlation length ξ for $P=1.2$, $\tau=48$, $\epsilon=0.14$, and $N=32$ rolls for the unperturbed system (a) and in the presence of noise of amplitude 1.25×10^{-4} (b).

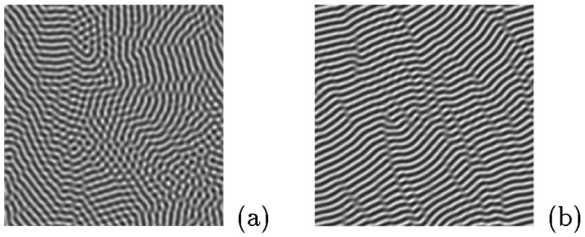

FIG. 5. Typical snapshots of convective patterns for $P=1.2$, $\tau=48$, $\epsilon=0.14$, and $N=32$ rolls at short time (a) and at long time (b), in the absence of noise.

entation, variable in time, and are transversally broken by KL fronts [Fig. 5(b)]. As seen from the time variation of the correlation length [Fig. 4(a)], the transition between these two phases is quite abrupt. The time-averaged correlation length considered in the following is computed on this latter regime.

Since the dynamics appears to be extremely unstable, we expect a strong sensitivity of the correlation length to the wall defects which form with realistic boundary conditions. In order to simply mimic their effect, we resorted, as a first step, to just add, a random noise to the SH type model. Its amplitude, probably larger than in the actual laboratory experiments, was taken as independent of ϵ (but decreasing with the size of the box), and sufficient to have a measurable effect while preserving the global structure of the patterns. We thus added to Eq. (1) a white noise, distributed on the Fourier modes in the wave number range $1\leqslant k\leqslant 20$ with a constant amplitude of order 10^{-4} (a comparable magnitude for the r.m.s. amplitude of the forcing is obtained in physical space). At the level of the correlation length, this perturbation strongly reduces the amplitude of the peaks, as seen conspicuously in Figs. 3 and 4 for $N=16$ and $N=32$, respectively. Note that for the latter resolution, the previously mentioned transition between the two phases is significantly delayed in the presence of noise, which tends to inhibit the relaminarization. An effect analogous to the reduction of the peak amplitude is the variation of the correlation length with

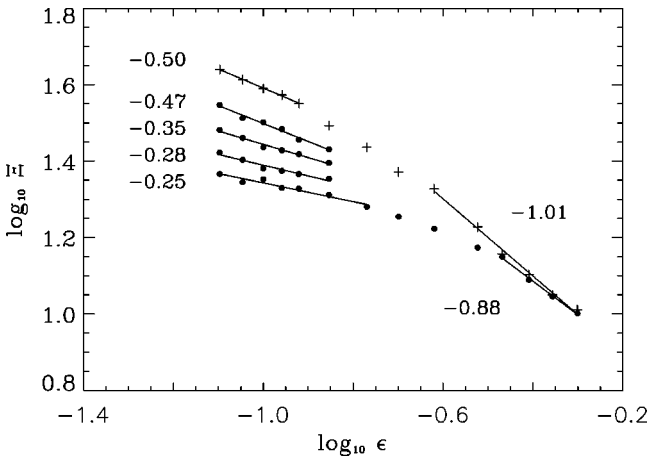

FIG. 6. Time-averaged correlation length Ξ vs ϵ for $\tau=48$ and $N=16$ rolls without noise (crosses) and with a random noise (bullets) of amplitudes 1.25×10^{-4}, 2.5×10^{-4}, 3.75×10^{-4}, and 5.0×10^{-4} (from top to bottom). Curves are labeled by the corresponding slope.

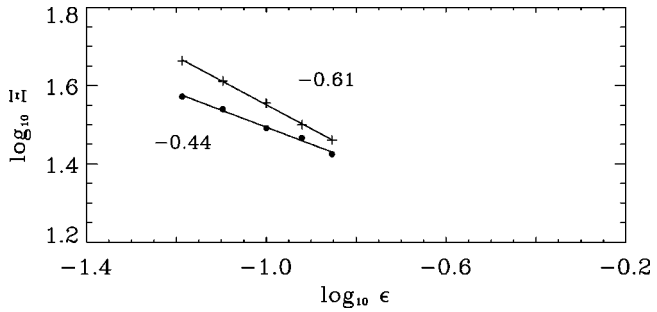

FIG. 7. Time-averaged correlation length Ξ vs ϵ for $\tau=48$ and $N=32$ rolls without noise (crosses) and with a random noise of amplitude 1.25×10^{-4} (bullets).

the rotation rate τ, which for τ close to τ_{KL} presents a maximum much sharper in the simulations (Fig. 3 of [9]) than in the laboratory experiments (Fig. 28 of [2]).

As can be seen in Figs. 6 and 7, we also observe that varying the noise amplitude has a strong effect (depending on the number of rolls) on the scaling of the time-averaged correlation length Ξ with ϵ. In the absence of noise and at small ϵ the scaling exponent is close to -0.5 in the simulations with $N=16$ (Fig. 6). In this setting, as the noise amplitude is increased, the slope becomes shallower and, for a noise amplitude of 5×10^{-4} [whose blurring effect on the pattern is visible in Fig. 8(a)], it approaches -0.25 ± 0.04. This value is compatible with the experimental results presented in [2,3], although the range of values of ϵ accessible in the simulations is much more limited than in the laboratory experiments. At larger ϵ, we find an exponent approaching -0.88 ± 0.05, slightly in excess of the experimental determination, the difference possibly originating from the fact that SH type models are not expected to be accurate far from onset.

When increasing the number of rolls to $N=32$, a sizeable effect on the scaling of the correlation length requires a much weaker noise amplitude. An exponent -0.61 ± 0.00 is obtained in the absence of noise and it becomes -0.44 ± 0.01 with a noise of amplitude 1.25×10^{-4} (Fig. 7). In this case, the resulting blurring effect on the pattern is rather weak [Fig. 8(b)]. We note that, when measured in the same ϵ range, the slope obtained in the absence of noise is steeper for $N=32$ than for $N=16$. This effect is understood by noticing that varying both the system size and the value of ϵ according to the scaling law governing the correlation length leads to qualitatively similar patterns [4]. The values of ϵ considered with $N=32$ thus correspond to larger effective values in the simulations with $N=16$ and fall in a range

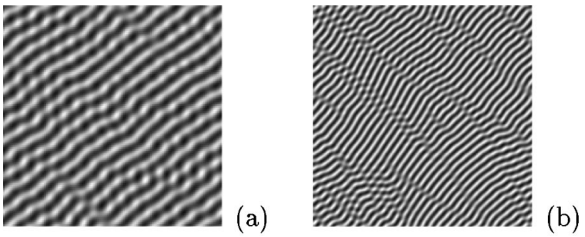

FIG. 8. Typical snapshots of convective patterns for $P=1.2$, $\tau=48$, and $\epsilon=0.1$ in the presence of a noise of amplitude 5×10^{-4} for $N=16$ rolls (a) and amplitude 1.25×10^{-4}, $N=32$ rolls (b).

where the correlation length decays faster. A slope close to -0.5 for $N=32$ would require smaller values of ϵ, for which reliable statistics request extremely long computations.

To summarize, in our simulations the correlation length is observed to vary as a power law with respect to the distance to threshold. When considered in the same range of ϵ, the exponent is affected by both the number of rolls in the convection cell and the random noise used to mimic the isolated defects created by the lateral walls. A sensitivity of scaling exponents to the amplitude of the noise was already noticed in simulations of the usual SH equation in the absence of rotation [13]. In this context, the correlation increases continuously in time like a power law. The corresponding exponent was obtained to be 1/5 in the absence of noise and 1/4 with a noise of amplitude 0.05. A regime with an exponent 1/2 is eventually expected after all the isolated defects have been eliminated. In both the rotating and nonrotating problems, the noise affects the density of isolated defects which influences the scaling exponents, making their value nonuniversal. In rotating convection, defects are, however, continuously formed as a consequence of the KL instability, and nonuniversality is thus expected to persist.

The question remains as to the role of the Prandtl number. Preliminary simulations at infinite Prandtl number indicate that a random noise twice as strong is necessary to exert a visible influence on the correlation length, probably because of the absence of a mean flow, known to induce a more chaotic dynamics.

Computer facilities were provided in part by the Program ''Simulations Interactives et Visualisation en Astronomie et Mécanique (SIVAM).''

[1] G. Küppers and D. Lortz, J. Fluid Mech. **35**, 609 (1969).
[2] Y. Hu, R. E. Ecke, and G. Ahlers, Phys. Rev. E **55**, 6928 (1997).
[3] Y. Hu, W. Pesch, G. Ahlers, and R. E. Ecke, Phys. Rev. E **58**, 5821 (1998).
[4] M. C. Cross, D. Meiron, and Y. Tu, Chaos **4**, 607 (1994).
[5] Y. Ponty, T. Passot, and P. L. Sulem, Phys. Rev. E **56**, 4162 (1997).
[6] P. Manneville, J. Phys. (France) **44**, 759 (1983).
[7] S. W. Morris, E. Bodenschatz, D. S. Cannell, and G. Ahlers, Phys. Rev. Lett. **71**, 2026 (1993).
[8] M. C. Cross, Physica D **97**, 65 (1996).
[9] Y. Ponty, T. Passot, and P. L. Sulem, Phys. Rev. Lett. **79**, 71 (1997).
[10] F. H. Busse and K. E. Heikes, Science **208**, 173 (1980).
[11] F. H. Busse, in *Turbulence and Chaotic Phenomena in Fluids*, edited by T. Tatsumi (Elsevier, Amsterdam, 1984), p. 197.
[12] Y. Tu and M. C. Cross, Phys. Rev. Lett. **69**, 2515 (1992).
[13] K. R. Elder, J. Viñals, and M. Grant, Phys. Rev. Lett. **68**, 3024 (1992).